Solid State Science and Technology, Vol. 33, No. 1 (2025) 14-24
https://doi.org/10.66514/ssst33-1-14-24

Temperature Coefficient of Resistivity for Doped Manganites Towards Sustainability of Magnetic Based Temperature Sensor

Nur Iezzatie Alya Binti Zamri[1], Muhammad Harith Syaqawi Bin Mohd Fadil[1], Muhammad Arif Syazwan Bin Nor Akbal[1], Mohammad Afiq Ikhwan Bin Zainuddin[1], Rozilah Rajmi[2], Nor Nurkhaizan Zulkepli[3], Masnita Mat Jusoh[3], Norazila Binti Ibrahim[1,]*

[1]Faculty of Applied Sciences, Universiti Teknologi MARA (UiTM], 40450 Shah Alam Selangor, Malaysia

[2]Faculty of Applied Sciences, Universiti Teknologi MARA (UiTM], Perlis Branch, Arau Campus, 02600 Arau, Perlis, Malaysia

[3]Centre of Foundation Studies, Universiti Teknologi MARA, Selangor Branch, Dengkil Campus 43800 Dengkil, Selangor, Malaysia

**Corresponding author: noraz954@uitm.edu.my*

(Received: 25 March 2025 / Revised: 3 June 2025 / Accepted: 7 June 2025 / Published online: 20 June 2025)

ABSTRACT

The temperature coefficient of resistivity (TCR] in perovskite manganite ceramics is a key parameter that characterizes the sensitivity of resistivity to temperature changes. However, many studies report that these materials typically exhibit a low TCR peak temperature (T_k] and limited maximum TCR values, which restricts their practical applications. Notably, the resistivity of these materials increases sharply near the metal-insulator transition temperature, T_{MI} leading to a significant rise in TCR. This unique behavior has been attributed to MnO_6 distortion, indicating that further research is needed to clarify the role of lattice distortion in influencing TCR. To explore this, $La_{0.8-x}M_xNa_{0.2}MnO_3$ (M=Eu^{3+}, Dy^{3+}, Er^{3+}, x=0, 0.1] monovalent-doped manganites was prepared using the solid-state reaction method, aiming to investigate how lattice distortion affects TCR. Specifically, we focused on the substitution of smaller ionic radius elements, such as Eu^{3+} (1.12 Å], Dy^{3+} (1.07 Å] and Er^{3+} (0.89 Å] compared to La^{3+} (1.216 Å). Our findings revealed that all substituted samples exhibited a metal-insulator transition with an increase in resistivity. In contrast, the parent sample exhibited metallic behavior across the entire measured temperature range of 30 K to 300 K with lower resistivity than the substituted samples. Interestingly, our results indicate that TCR values are significantly influenced by the type of elemental substitution. The maximum TCR increased from 0.83 % K^{-1} at ~118 K for the x=0 sample to 0.93 % K^{-1} at ~220 K for the

Dy-substituted sample, 1.012 % K^{-1} at ~280 K for the Er-substituted sample and 6.21 % K^{-1} at 260 K for Eu-substituted sample. These findings highlight the impact of rare earth element substitution on the transformation of manganites from a ferromagnetic metal to a paramagnetic insulator and the corresponding MnO_6 octahedral distortion as well as on TCR values, making these materials promising for advanced uncooled device applications.

Keywords: Manganites; resistivity; temperature coefficient of resistance (TCR).

INTRODUCTION

Manganite materials exhibit ferromagnetic metallic (FMM) to paramagnetic insulating (PMI) transition behaviour with transition temperature represented by the value of T_c for ferromagnetic to paramagnetic transition behaviour and T_{MI} for metal to insulating transition behaviour. The observation of such fascinating behaviour was widely reported in divalent doped manganite [1-3]. The observed metal to insulating transition behaviour was believed as a result of combination of scattering effect on electron charge carriers, e_g and MnO_6 lattice distortion effect as temperature increases. In addition to that, the magnetic interaction between manganese ions (Mn^{3+} and Mn^{4+}) was also attributed to the fascinating properties observed in manganite such as electrical properties [1-3], magnetoresistance (MR) effect [1-3], electroresistance (ER) effect [4,5] and temperature coefficient resistance (TCR) [6-10].

The temperature coefficient of resistivity (TCR) reflects the sensitivity of materials to the change of temperature and the value of TCR can be determined as follows [6-10]:

$$\text{TCR } \% = [1/\rho \times (d\rho/dT)] \times 100\% \quad (1)$$

Based on eq. (1), TCR value is related to two variables: inverse of resistivity of the investigated samples, $1/\rho$ and changes of resistivity as a result of change of temperature, $d\rho/dT$. Based on the equation, it is understood that the sample which exhibit low resistivity and exhibit rapid change of resistivity to the change of temperature is expected to exhibit high TCR value. In manganites, both parameters of resistivity, ρ and dρ/dT was reported can be influenced by lattice distortion effect [6] indicate the TCR effect have a strong link with lattice distortion. For instance, in divalent doped manganites, such as $La_{0.7-x}Eu_xSr_{0.3}MnO_3$ (x=0, 0.1, 0.2, or 0.3), substitution of Eu which is smaller average ionic radius (1.12 Å) compared to La at the A-site reduce the metal-insulator transition temperature, T_{MI} value from 390 K (x=0) to 240 K (x=0.3), but the substitution enhanced the maximum TCR value from 1.1 % (x=0) to 1.9% (x=0.2) and 3.36% (x=0.3) The observed behaviour was suggested due to the enhancement of lattice distortion effect as indicated by the reduction of unit cell volume attributed to the reduction of average ionic radius at A-site, $\langle r_A \rangle$ as a result of Eu substitution. Further, Chu et al. (2022), found that the TCR values in $La_{0.8-x}Sr_xAg_{0.2}MnO_3$ (LSAMO, x=0.00, 0.10, 0.15, 0.175) are affected by the amount of doped Sr [11]. The values increased from 2.5 % K^{-1} for $La_{0.8}Ag_{0.2}MnO_3$ at 211.5 K to 16.9 % K^{-1} for $La_{0.625}Sr_{0.175}Ag_{0.2}MnO_3$ at 299.8 K which are also attributed to lattice distortion effect [11]. Finally, for $La_{0.8}Sr_{0.2-x}K_xMnO_3$ the maximum TCR value is 9.11% K^{-1} at 292.44 K for x=0.08 compared to 6.03% K^{-1} at 266.57 K for x=0.02 [12] indicating TCR value can be further increased because of increased of substituent

concentration.

Interestingly, TCR was also reported in $La_{1-x}Na_xMnO_3$ (LNMO) monovalent doped manganites. TCR value increases from 5.89 % K^{-1} at x=0.1 to 8.56 % K^{-1} at x=0.4. The peak of TCR reached 299.42 K. Possible reasons for the observed TCR effect was suggested as a combination of grain boundary effect, A-site mismatch effect, double-exchange mechanism and the inducement of Jahn–Teller distortions [8]. Therefore, it is interesting to further investigate the role of lattice distortion in $La_{0.8(1-x)}M_xNa_{0.2}MnO_3$ (M=Dy^{3+}, Eu^{3+} and Er^{3+}, x=0.0, 0.1) monovalent doped manganites as a result of substitution by different type of elements. Substitution of Dy at the La-site in $La_{0.7-x}Dy_xSr_{0.3}MnO_3$ induced lattice distortion effect as a result of smaller ionic radius of Dy^{3+} (1.07 Å) and influence the resistivity and the changes of resistivity to the temperature [13]. Furthermore, Er substitution at La-site in $La_{0.7-x}Er_xCa_{0.3}MnO_3$ induced lattice distortion and weakened double exchange (DE) mechanism as the ionic radius of Er^{3+} (0.89 Å) smaller compared to La^{3+} (1.21 Å) [14]. When Er substitutes La, the mismatch in ionic radius causes significant lattice distortions, which impact the Mn–O–Mn bond angles and distances which affecting the DE interactions. Therefore, based on above mentioned matter, the substitution of Dy^{3+}, Eu^{3+} and Er^{3+} in $La_{0.8(1-x)}M_xNa_{0.2}MnO_3$ is expected to contribute to the different degree of lattice distortion effect as a result of different of average of ionic radius at A-site and as a consequence the resistivity behaviour and slope resistivity versus temperature (ρ-T) curve may be different among the investigated samples.

MATERIALS AND METHODS

Sample preparation

Polycrystalline bulk samples of $La_{0.8(1-x)}M_xNa_{0.2}MnO_3$ (M = Dy, Eu, Er and x = 0.1) were synthesized using solid state method. High purity La_2O_3, Na_2CO_3, Eu_2O_3, Er_2O_3, Dy_2O_3 and MnO_2 were selecting as starting materials and mixed in the appropriate stochiometric ratios. The powders were ground for 2 h and calcined for 24 h at 950 °C. The calcined powders were then reground, pelletized and sintered at 1050 °C for 48 h. After the first sintering, the samples were crushed again, reground into fine powder for 2 h and then pressed into pellets. The samples were sintered for a second time at 1150 °C for 72 h with slow cooled to room temperature.

The phase formation of prepared samples in fine powder form is investigated using Rigaku X-Ray diffractometer PAN Analytical model Xpert PRO with CuK_α (λ=0.154 nm) radiation at room temperature in the range of 2θ from 20° to 90°. The Rietveld refinement method, utilizing the GSAS, EXPGUI and VESTA software, is employed for further analysis of phase formation and the determination of structural parameters. The surface morphologies of the investigated samples were examined using a LEO model 982 Gemini Scanning electron microscopy (SEM) with magnification of ×5k. The temperature dependent electrical resistance measurement is carried out using standard four-point probe technique in a Janis model CCS 350ST cryostat 350ST and controlled by a Lake Shore Model 330 temperature controller in the temperature range of 30-300 K. The sample in the pellet form were placed on a sample holder. Four thin lead wires with two pairs of current and voltage wires were attached to the sample using a conductive silver paste to ensure good electrical contact between the wires and sample. Current is supplied by a Keithly 224 Programmable Current Source, and the voltage drop was measured by a Keithly 2010 multimeter. The measurement of ac susceptibility as a function of temperature was carried out using a closed cycle refrigerator Model 350CP controlled by a Lake Shore Model 335 temperature controller from 30 K to 310 K. The samples were prepared in a fine powder form and placed inside a capsule, before being

attached at the end of the sample holder. The resultant signal is measured using a DSP Lock-In Amplifier Model 7265 with the in phase and out phase components of the signal.

RESULTS AND DISCUSSION

X-ray diffraction (XRD) analysis

Figure 1 represents the XRD patterns for all samples for 2θ=10º to 90º at room temperature. For the parent compound (x=0), the diffraction pattern is found to be similar to the report by Kansara et al. [15]. The finding indicate good quality of prepared samples without the detection of impurity phases. Both Dy- and Eu-substituted samples exhibit a similar XRD pattern while for Er-substituted samples showed a small impurity peak is shown in the X-ray diffraction pattern. The X-ray diffraction data were further refined through Rietveld refinement technique using GSAS, EXPGUI and VESTA software.

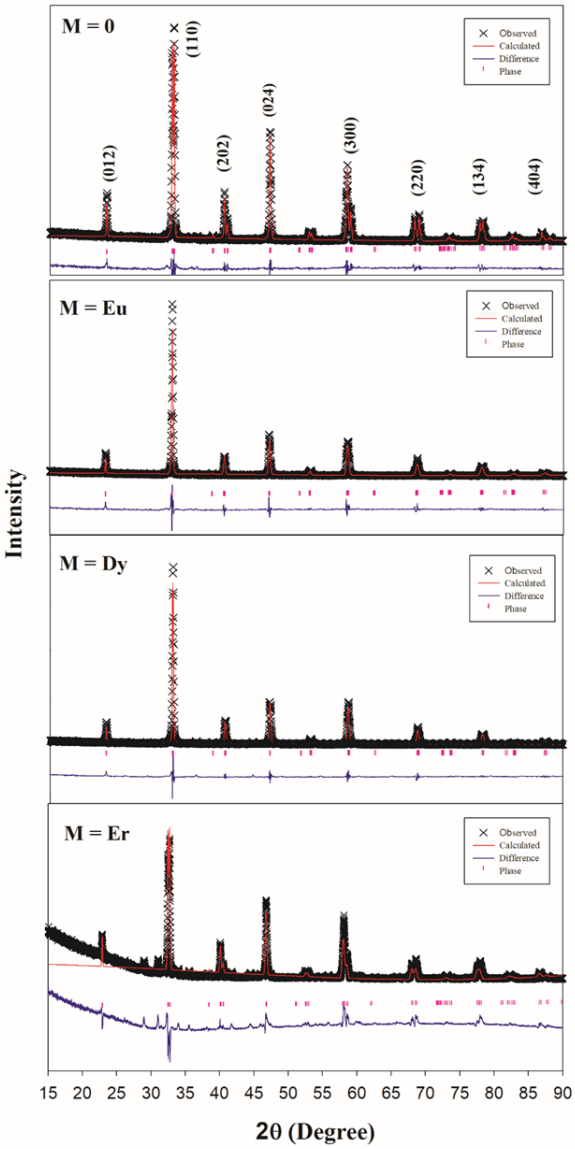

Figure 1. X-ray diffraction pattern for $La_{0.8}Na_{0.2}MnO_3$, $La_{0.7}Eu_{0.1}Na_{0.2}MnO_3$, $La_{0.7}Dy_{0.1}Na_{0.2}MnO_3$ and $La_{0.7}Er_{0.1}Na_{0.2}MnO_3$ for 2θ=10º to 90º

The final refinement values of the structural parameters, chi-squared (χ^2), average ionic radius, tolerance factor, and variance for all samples are shown in Table 1. It clearly shows a decrease in unit cell volume with the substitution of Eu^{3+} and Dy^{3+}, and an increase in the Er^{3+} sample. It can be seen that the calculated average ionic radius ($<r_A>$), tolerance factor (τ), and variance (σ^2) decrease with the substitution of Eu^{3+}, Dy^{3+}, and Er^{3+} (Table 1). The τ is 0.9336 nm for $La_{0.8}Na_{0.2}MnO_3$, and it decreases to 0.9301 nm ($La_{0.7}Eu_{0.1}Na_{0.2}MnO_3$), 0.9283 nm ($La_{0.7}Dy_{0.1}Na_{0.2}MnO_3$), and 0.9219 nm ($La_{0.7}Er_{0.1}Na_{0.2}MnO_3$) which indicates that the compounds are in a stable perovskite structure and crystallize in the orthorhombic structure. The slight decrease in unit cell volume with Eu^{3+} and Dy^{3+} substitution suggests that Eu^{3+} and Dy^{3+} may replace La^{3+} because the ionic radii of Eu^{3+} (1.12 Å) and Dy^{3+} (1.07 Å) are smaller than that of La^{3+} (1.216 Å). However, for Er^{3+} substitution, the unit cell volume is unexpectedly larger, even though Er^{3+} (0.89 Å) is smaller than both Eu^{3+} and Dy^{3+}. This may be due to impurities in the sample, which affected the refinement analysis and consequently influenced the structural parameter values.

Table 1: Structure parameters obtained by Rietveld Refinement, average ionic radius at the A-Site ($<r_A>$), tolerance factor (τ) and variance (σ^2) of $La_{0.8}Na_{0.2}MnO_3$, $La_{0.7}Eu_{0.1}Na_{0.2}MnO_3$, $La_{0.7}Dy_{0.1}Na_{0.2}MnO_3$ and $La_{0.7}Er_{0.1}Na_{0.2}MnO_3$ manganites

Sample	$La_{0.8}Na_{0.2}MnO_3$	$La_{0.7}Eu_{0.1}Na_{0.2}MnO_3$	$La_{0.7}Dy_{0.1}Na_{0.2}MnO_3$	$La_{0.7}Er_{0.1}Na_{0.2}MnO_3$
Lattice parameter *a* (Å)	5.512887(162)	5.494269(918)	5.48015(37)	5.50914(122)
b (Å)	5.512887(162)	5.494269(918)	5.48015(37)	5.50914(122)
c (Å)	13.34778(462)	13.42629(761)	13.4001(180)	13.3532(307)
Volume, *V* (Å^3)	351.316(026)	351.000(122)	348.517(22)	350.982(201)
Good fitness, χ2	2.48	3.87	5.49	30.41
Average ionic radius, $<r_A>$ (Å)	1.2088	1.1992	1.1942	1.1762
Tolerance factor, τ (nm)	0.9336	0.9301	0.9283	0.9219
Variance, σ^2($\times10^{-2}$ Å^2)	0.0207	0.0899	0.1916	0.9330

Scanning electron microscope (SEM) analysis

The Scanning Electron Microscope (SEM) micrographs in Figure 2 show the surface of $La_{0.8-x}M_xNa_{0.2}MnO_3$ samples (M = Dy, Eu and x = 0, 0.1). It is noticed that the microstructure such as grain shape and grain size not much change as a result of substitutions thus the observed electrical and TCR effect in this present investigation is suggested dominantly as a result of lattice distortion effect.

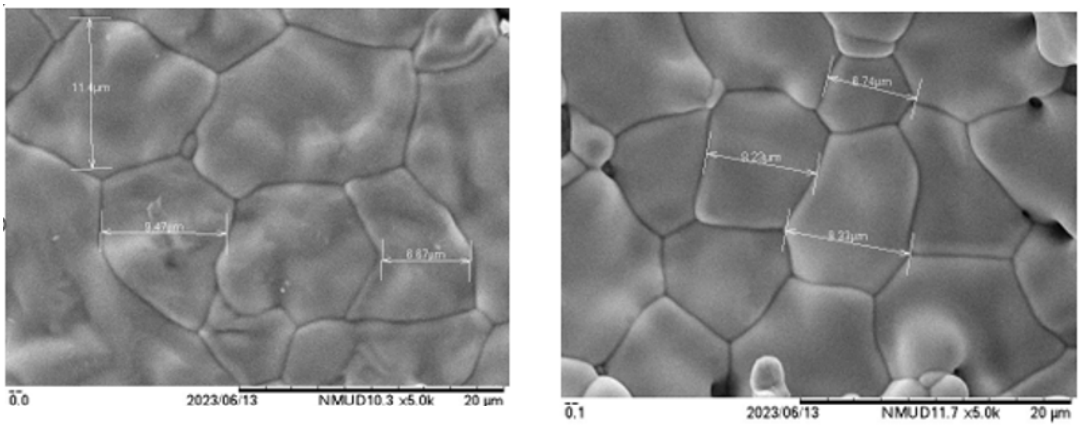

(a) (b)

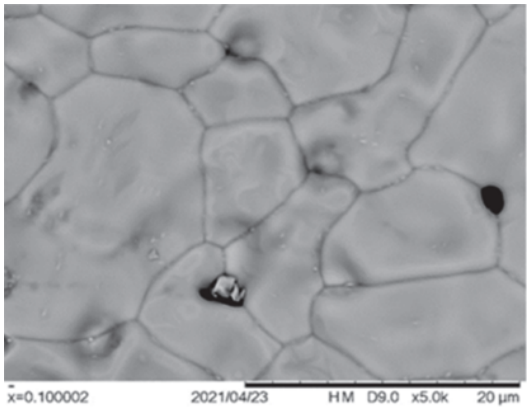

(c)

Figure 2. Scanning Electron Micrograph with magnification of 5k for (a) $La_{0.8}Na_{0.2}MnO_3$, (b) $La_{0.7}Eu_{0.1}Na_{0.2}MnO_3$ and (c) $La_{0.7}Dy_{0.1}Na_{0.2}MnO_3$

Electrical properties

Figures 3(a)–3(d) show the resistivity versus temperature for $La_{0.8-x}M_xNa_{0.2}MnO_3, (x = 0.0\ and\ 0.1)$, under applied current of 5 mA. As can be seen in Figure 3, the resistivity (ρ) vs. temperature (T) curve displays a metallic behaviour for x=0 sample across the whole temperature range of 20 K to 300 K. However, all substituted samples exhibit metal-insulating transition behaviour with increased in resistivity. Resistivity (ρ) vs. temperature (T) curves show that for Dy substituted sample, the value of metal-insulator transition temperature, T_{MI} is 220 K, while for Eu substituted sample the T_{MI} value increased to 260 K and for Er substituted sample, the T_{MI} is ~300 K. Among the substituted samples, $La_{0.7}Dy_{0.1}Na_{0.2}MnO_3$ exhibits the highest resistivity values and a broader range of insulating behaviour, suggesting a weakening of the double exchange process and an enhancement of charge carrier localization, which indicates strong electron-lattice interaction. The intensification of lattice distortion as indicated by the lowering of unit cell volume as shown in Table 1 owing to Dy substitution strongly weakened the double exchange mechanism.

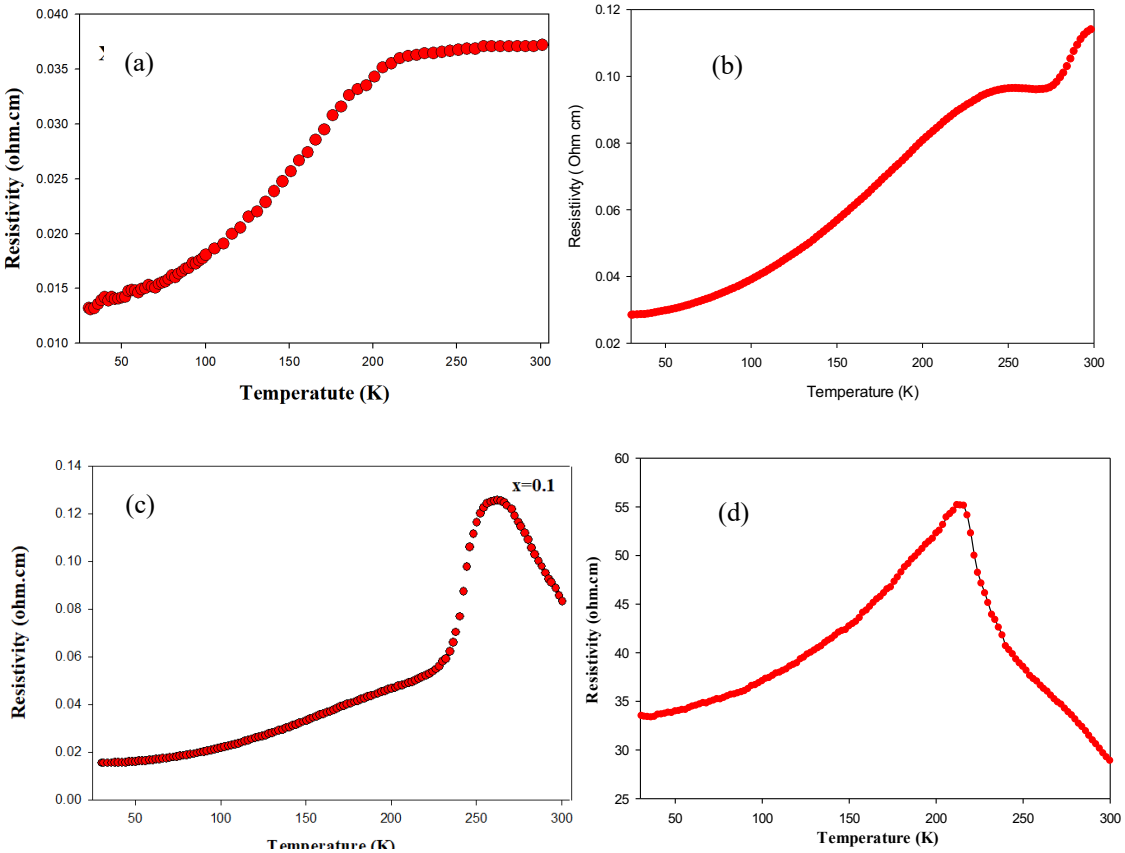

Figure 3. Resistivity (ρ) versus temperature (T) for (a) $La_{0.8}Na_{0.2}MnO_3$, (b) $La_{0.7}Er_{0.1}Na_{0.2}MnO_3$, (c) $La_{0.7}Eu_{0.1}Na_{0.2}MnO_3$ and (d) $La_{0.7}Dy_{0.1}Na_{0.2}MnO_3$

Magnetic properties

Figure 4(a) shows the real part of the ac susceptibility *vs*. temperatures of $La_{0.7}M_{0.1}Na_{0.2}MnO_3$ (M= Er, Eu, Dy) with fixed concentrations of the rare earth ion. The measurements were performed in a magnetic field of 2 Oe and at a frequency of 345 Hz. It is noted the unsubstituted sample exhibit long range of ferromagnetic (FM) region in the whole measured temperature region from 30 K to 300 K which indicates its strong ferromagnetic properties. However, the long range of ferromagnetic region is reduced indicating that the substitution of M=Er, Eu, and Dy weakened the ferromagnetic properties of the parent sample. Further, all substituted samples exhibit a transition from ferromagnetic to paramagnetic (PM) behaviour with reduction of transition temperature, Tc=291 K(Er-substituted sample), Tc=245 K (Eu-substituted sample) to Tc=193 K (Dy-substituted sample. The Curie temperature, T_C, for all samples is determined form minimum point of the $d\chi'/dT$ *vs*. T curves as shown in Figure 4 (b).

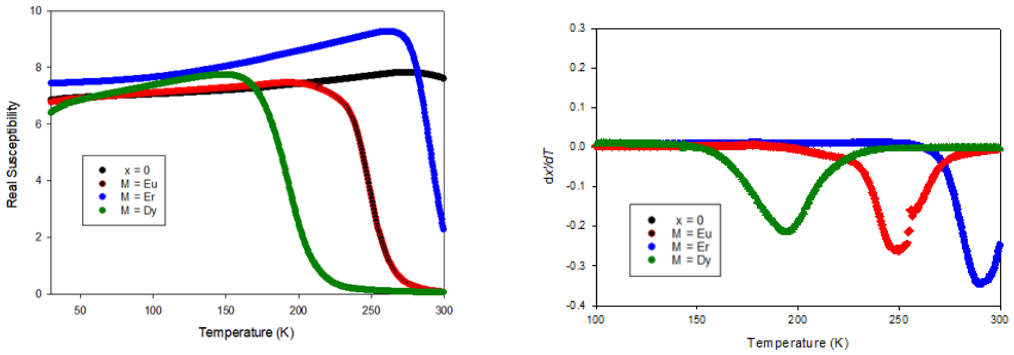

(a) (b)

Figure 4. (a) The real part of ac susceptibility, χ' vs. *T* for $La_{0.8-x}M_{0.1}Na_{0.2}MnO_3$ (M=Eu, Er, Dy) and (b) The $d\chi'/dT$ vs. *T* curves for $La_{0.8-x}M_{0.1}Na_{0.2}MnO_3$ (M=Eu, Er, Dy).

The findings show that substitution at La-site by smaller rare-earth ions led to the weakening of ferromagnetic properties of the substituted samples in $La_{0.7}M_{0.1}Na_{0.2}MnO_3$ (M= Er, Eu, Dy. The variation in the magnetic properties as a result of substitution is believe have a strong relation with the different degree of lattice distortion due to different ionic radius of Eu, Er and Dy. The substitution of these rare earth ions does not alter the ratio of Mn^{3+}/ Mn^{4+} ions due to same valence state with La^{3+} but results in a more distorted structure result of occurrence of mismatch effect indicating by larger value of σ^2 and shorter average A site-ionic radius ($<r_A>$) in substituted samples compared to unsubstituted sample (Table 1). Decreasing the average A-site ionic radius ($<r_A>$) led to reduced Mn–O–Mn-bond length and angle, enhanced spin disordering between Mn ions [6,13,14], and consequently, the FM-metallic (FMM) phase was diminished by the substitution. This will affect the transfer integral of e_g electron hopping between Mn sites, which consequently reduces the strength of DE involving Mn^{3+} –O^{2-}– Mn^{4+} interactions and suppression of the ferromagnetism which causes decrease in *Tc* value.

Temperature coefficient of resistance (TCR) effect

TCR (%) for all investigated samples in temperature range from 20 K to 300 K are shown in Figure 5(a) – 5(d). For the x=0 sample, TCR value increased in the temperature range of 30 K to 120 K and gradually decrease to 300 K before remaining almost constant in the temperature range of 260 K to 300 K, with the maximum value of TCR being 1.13% at ~116 K. Interestingly, Eu substituted sample exhibit TCR maximum value of 6 % at 220 K and negative TCR value in the temperature range of 250 K to 300 K. The observed behaviour indicates that high operating temperature and enhancement of TCR effect can be achieved by Eu substitution at La-site in $La_{0.7}Eu_{0.1}Na_{0.2}MnO_3$. Further, for Dy substituted sample, TCR maximum with value of 0.93 % is observed at T ~ 220 K which is lower that Eu substituted sample. While for Er substituted sample, TCR maximum is observed with value of 1.1 % near to 290 K.

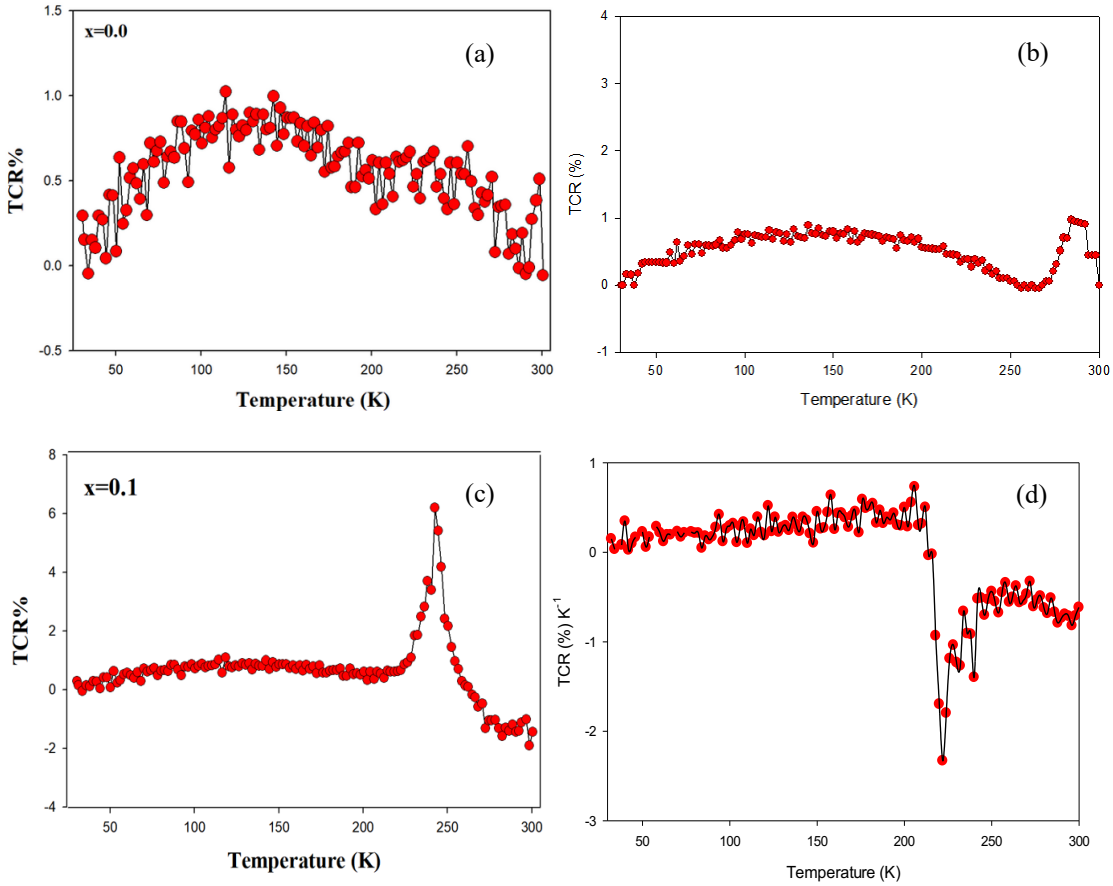

Figure 5. TCR (%) with temperature for (a) $La_{0.8}Na_{0.2}MnO_3$, (b) $La_{0.7}Er_{0.1}Na_{0.2}MnO_3$, (c) $La_{0.7}Eu_{0.1}Na_{0.2}MnO_3$ and (d) $La_{0.7}Dy_{0.1}Na_{0.2}MnO_3$

Our finding shows that the TCR maximum can be obtained in the vicinity of the metal-insulating transition temperature indicating dominant effect of $\frac{d\rho}{dT}$. In this temperature region, the slope of the resistivity versus temperature (ρ-T) curve is greater as compared to other temperature region. According to the following equation of TCR (%)=1/ρ dρ/dT×100%, TCR would fall as resistivity increased. As a result of the rise in resistivity, which leads to a smaller value of $1/\rho$, the slope of the ρ vs T curve, which is represented by the term of $d\rho/dT$, may have less of an impact in this situation.

On the other hand, the higher TCR effect brought on by the Eu substitution at the vicinity of metal-insulating transition temperature may be primarily the result of lattice distortion, which in turn increased the change in resistivity as the temperature raised and, as a result, raised the value of $d\rho/dT$. Thus, $d\rho/dT$ became dominance as compared to $1/\rho$. In this case, it seems that the change of resistivity with temperature occurred very fast at the vicinity of metal-insulator transition temperature which contribute to the high sensitivity of the material to the change of temperature. The main factor may be due to the increase of lattice distortion effect as temperature increase thus, contributing to sudden increase in resistivity. On the other hand, above T_{MI}, the TCR effect drop to negative value in the semiconducting region which reflecting its semiconducting like behavior.

Further, the observed smaller value of TCR maximum for Er-substituted as compared to Eu-substituted sample may be related to smaller $\frac{d\rho}{dT}$ of the latter as compared to the former. Further, Dy substituted samples exhibit smallest value of TCR maximum among the investigated sample may be related to dominant effect of $1/\rho$ value which smallest as the sample exhibit highest value of resistivity among the investigated sample. Dy substitution is suggested to induce strong lattice distortion effect as indicated by large value of mismatch effect and smallest value of unit cell volume thus led enhancement of blocking effect of charge carrier hence result to large of increased of resistivity.

CONCLUSION

In summary, we have investigated the influence of partial substitution of La by smaller ionic radii rare-earths elements in $La_{0.8-x}M_xNa_{0.2}MnO_3$ compounds. The Rietveld refinement of the X-ray data confirms that the M (M= Dy, Eu, Er) elements successfully substitute the La-site in the $La_{0.8}Na_{0.2}MnO_3$ compound which is reflected by the reduction of the unit cell volume. The substitution of La by smaller radii ionic radii RE elements ($La_{0.8-x}M_xNa_{0.2}MnO_3$) reduced the average effective radii of A-site, which alter degree of MnO_6 distortion. All substituted samples exhibit metal-insulator transition behaviour with increased in resistivity, indicating the existence of Jahn-Teller distortion. Most importantly, the TCR enhance significantly with rare-earth doping in the $La_{0.8-x}M_xNa_{0.2}MnO_3$ system. The maximum TCR value was observed near to T_{MI} indicating the large sensitivity of material to temperature in manganites is related to rapid change of resistivity to temperature which arise due to lattice distortion effect.

REFERENCES

1. Purnakanti A, Manendar M, Kumar S, Venkatesh R, Lakshmi YK, Reddy MS. Magneto transport behaviour of $La_{0.67}Pb_{0.33}MnO_3$ manganites system with various additives. *J Solid State Chem*. 2023;324:124112.
2. Choudhary YRS, Mangavati S, Patil S, Rao A, Nagaraja BS, Thomas R, et al. Effect of rare earth substitution at La site on structural, electrical and thermoelectric properties of $La_{0.7-x}RE_xSr_{0.3}MnO_3$ (x = 0, 0.2, 0.3; RE = Eu, Gd, Y). *J Magn Magn Mater*. 2018;451:110–20.
3. Vitayaya O, Nehan PZZ, Munazat DR, Manawan MTE, Kurniawan B. Magnetoresistance (MR) properties of magnetic materials. *RSC Adv*. 2024;14(16):18617–45.
4. Zahrin A, Ibrahim N, Mohamed Z. Effects of Li substitution on structural, magnetic properties and electroresistance behaviour in $La_{0.8}Na_{0.2-x}Li_xMnO_3$ monovalent doped manganite. *J Mater Sci Eng B*. 2023;295:118813.
5. Ibrahim N, Sazali MS, Mohamed Z, Rozilah R. The effects of Mo partial substitution at the Mn site on electroresistance behavior in $La_{0.7}Ba_{0.3}Mn_{1-x}Mo_xO_3$ (x = 0–0.04) manganites. *J Electron Mater*. 2022;52:237–50.
6. Vadnala S, Rao TD, Pal P, Asthana S. Study of structural effect on Eu substituted LSMO manganites for high temperature coefficient of resistance. *Phys B Condens Matter*. 2014;448:277–80.
7. Debnath M, Biswas B, Bo E, Pal S. Structural, magnetic and magnetotransport

properties of $Pr_{0.5}Ca_{0.5}Mn_{0.9}V_{0.1}O_3$: Indication of large field coefficient of resistance (FCR). *J Magn Magn Mater*. 2021;527:167738.
8. Jin S, Zhang S, Li H, Chu K, Yu X, Guan X, et al. A-site Na doping to enhance room temperature TCR of $La_{1-x}Na_xMnO_3$ polycrystalline ceramic. *Mater Today Commun*. 2021;28:102496.
9. Pu X, Li H, Chu K, Duan Y, Li Z, Liu X. $(Pr_{0.75}La_{0.25})_{0.7}Sr_{0.3}MnO_3$:$Ag_x$ ($0 \leq x \leq 0.25$) polycrystalline with room temperature TCR improvement for uncooled infrared bolometers. *Ceram Int*. 2020;46:19028–37.
10. Yu X, Jin S, Li H, Guan X, Gu X, Liu X. High room-temperature TCR and MR of $La_{1-x}Sr_xMnO_3$ films for advanced uncooled infrared bolometers and magnetic sensors. *Appl Surf Sci*. 2021;570:151221.
11. Chua K, Li H, Pu X, Guan X, Yu X, Jin S, et al. Bivalent Sr^{2+} doping to improve room temperature TCR of $La_{0.8-x}Sr_xAg_{0.2}MnO_3$ polycrystalline ceramics. *J Alloy Compd*. 2022;902:163691.
12. Li H, Chu K, Pu X, Zhang S, Dong G, Liu Y, Liu X. A-site K-doping to enhance room temperature TCR of polycrystalline $La_{0.8}Sr_{0.2}MnO_3$ ceramic. *J Alloy Compd*. 2020;847:156417.
13. Song Q, Wang G, Yan G, Mao Q, Wang W, Peng Z. Influence of the substitution of Sm, Gd and Dy in $La_{0.7}Sr_{0.3}MnO_3$ on its magnetic and electric properties and strengthening effect in room temperature CMR. *J Rare Earths*. 2008;26(6):821–6.
14. Zhang X, Zhang G. Influence of Er doping on La site on lattice effect of low field magnetoresistance of manganite $La_{0.7}Ca_{0.3}MnO_3$. *Integr Ferroelectr*. 2019;198:1–8.
15. Kansara SB, Dhruv D, Kataria B, Thaker CM, Rayaprol S, Prajapat CL, et al. Structural, transport and magnetic properties of monovalent doped $La_{1-x}Na_xMnO_3$ manganites. *Ceram Int*. 2015;41:7162–73.